Original Article | Cardiovascular Imaging

eISSN 2005-8330
https://doi.org/10.3348/kjr.2019.0230
Korean J Radiol 2020;21(2):192-202

Korean Journal of Radiology
KJR

Coronary Computed Tomography Angiography-Derived Fractional Flow Reserve in Patients with Anomalous Origin of the Right Coronary Artery from the Left Coronary Sinus

Chun Xiang Tang, PhD[1]*, Meng Jie Lu, MSc[1]*, Joseph Uwe Schoepf, MD[1, 2], Christian Tesche, MD[2], Maximilian Bauer, MD[2], John Nance, MD[2], Parkwood Griffith, BS[2], Guang Ming Lu, MD[1], Long Jiang Zhang, MD, PhD[1]

[1]Department of Medical Imaging, Jinling Hospital, Medical School of Nanjing University, Nanjing, China; [2]Division of Cardiovascular Imaging, Department of Radiology and Radiological Science, Medical University of South Carolina, Charleston, SC, USA

Objective: To examine the fractional flow reserve derived from computed tomographic angiography (CT-FFR) in patients with anomalous origin of the right coronary artery from the left coronary sinus (R-ACAOS) with an interarterial course, assess the relationship of CT-FFR with the anatomical features of interarterial R-ACAOS on coronary computed tomographic angiography (CCTA), and determine its clinical relevance.

Materials and Methods: Ninety-four patients with interarterial R-ACAOS undergoing CCTA were retrospectively included. Anatomic features (proximal vessel morphology [oval or slit-like], take-off angle, take-off level [below or above the pulmonary valve], take-off type, intramural course, % proximal narrowing area, length of narrowing, minimum luminal area [MLA] at systole and diastole, and vessel compression index) on CCTA associated with CT-FFR ≤ 0.80 were analyzed. Receiver operating characteristic analysis was performed to describe the diagnostic performance of CT-FFR ≤ 0.80 in detecting interarterial R-ACAOS.

Results: Significant differences were found in proximal vessel morphology, take-off level, intramural course, % proximal narrowing area, and MLA at diastole (all $p < 0.05$) between the normal and abnormal CT-FFR groups. Take-off level, intramural course, and slit-like ostium (all $p < 0.05$) predicted hemodynamic abnormality (CT-FFR ≤ 0.80) with accuracies of 0.69, 0.71, and 0.81, respectively. Patients with CT-FFR ≤ 0.80 had a higher prevalence of typical angina (29.4% vs. 7.8%, $p = 0.025$) and atypical angina (29.4% vs. 6.5%, $p = 0.016$).

Conclusion: Take-off level, intramural course, and slit-like ostium were the main predictors of abnormal CT-FFR values. Importantly, patients with abnormal CT-FFR values showed a higher prevalence of typical angina and atypical angina, indicating that CT-FFR is a potential tool to gauge the clinical relevance in patients with interarterial R-ACAOS.

Keywords: *Right coronary artery arising from the left coronary sinus; Computed tomographic angiography; Fractional flow reserve; Coronary vessel anomalies*

Received April 1, 2019; accepted after revision September 25, 2019.
This study was supported by The National Key Research and Development Program of China (2017YFC0113400 for L.J.Z.) and the National Natural Science Foundation of China (81830057 for L.J.Z and 81803338 for M.J.L).
*These authors contributed equally to this work.
Corresponding author: Long Jiang Zhang, MD, PhD, Department of Medical Imaging, Jinling Hospital, Medical School of Nanjing University, Nanjing, Jiangsu 210002, China.
• Tel: (86) 13405833176 • Fax: (86) 2580860185 • E-mail: kevinzhlj@163.com

Korean Journal of Radiology
KJR

INTRODUCTION

The overall detection rate of anomalous origin of a coronary artery from the opposite sinus (ACAOS) is 0.15–0.39% with catheter angiography and 0.35–2.1% with coronary computed tomographic angiography (CCTA) (1). ACAOS is divided into the following five types according to the course the anomalous artery takes to reach its dependent myocardial territory: interarterial, subpulmonic, pre-pulmonic, retroaortic, and retrocardiac (2, 3). An interarterial course is the abnormality most consistently associated with sudden cardiac death (SCD). Left ACAOS with an interarterial course is most commonly linked to SCD during or after intense exercise. However, anomalous origin of the right coronary artery (RCA) from the left coronary sinus (R-ACAOS) with an interarterial course, reported as the most common "malignant" coronary anomaly with a weighted prevalence of 0.23% and 0.32% on CCTA (3), is associated with myocardial ischemia and may even be the cause of syncope, arrhythmia, myocardial infarction, and SCD (4-6). Rational management of patients with this anomaly requires robust risk stratification for the potential of SCD (7).

CCTA has been shown to be superior to catheter angiography in delineating anomalous coronary arteries (8). However, only a few studies have attempted to use CCTA features to move beyond diagnosis to more formal risk stratification (6, 9). Invasive measurement of fractional flow reserve (FFR), the reference standard method to determine lesion-specific ischemia, was used to guide therapy of R-ACAOS patients in some cohort studies (10-14), but this method has seen limited clinical adoption due to its invasive nature and high cost. Recently, FFR derived from computed tomographic angiography (CT-FFR) has been developed based on computational fluid dynamics modeling or deep machine learning algorithms (15-18), and it has been used for non-invasively assessing lesion-specific ischemia and guiding revascularization and treatment strategies in patients with stable coronary artery disease (15). Two recent case reports have described severe inducible ischemia by using CT-FFR in R-ACAOS patients with an interarterial course that was confirmed by invasive FFR (19-20). However, the potential value of CT-FFR in this anomaly has not been systematically validated in larger cohort studies.

Thus, the purpose of this investigation was to examine the CT-FFR in R-ACAOS patients with an interarterial course, assess its relationship with the anatomical features observed on CCTA, and determine its clinical relevance.

MATERIALS AND METHODS

Study Protocol and Patient Population

This retrospective study was approved by the Institutional Review Board of our hospital. The requirement for written informed consent was waived. From September 1, 2009 to November 31, 2017, a total of 41580 consecutive patients underwent CCTA. In this population, 527 patients (1.3%) showed anomalous origin of the left coronary artery or RCA. Of these 527 patients, 121 (23.0%) had R-ACAOS with an interarterial course, with a prevalence of 0.29% (121/41580). The exclusion criteria were as follows: more than 50% luminal stenosis in any epicardial coronary artery (n = 16), valvular heart disease (n = 4), left coronary artery dominance (n = 2), coronary arterial fistula (n = 1), or poor image quality unsuitable for CT-FFR analysis (n = 4). A flowchart of this study is provided in Supplementary Figure 1.

Relevant demographic characteristics, clinical history, and test results, including the findings of resting electrocardiography (ECG) and creatine kinase (CK) and CK-myocardium-brain type (MB) measurements, were collected for each patient via electronic medical record review. We classified patients according to the characteristics of chest pain as follows: typical, atypical, nonanginal, and no chest pain. According to the European Society of Cardiology guidelines, typical angina was defined as follows: 1) substernal chest discomfort with a characteristic quality and duration that is 2) provoked by exertion or emotional stress, and 3) relieved by rest or nitroglycerin (21). Atypical angina was defined as chest discomfort that did not show one of the above characteristics, and nonanginal chest pain was defined as chest discomfort that showed one or none of the typical angina characteristics. Patients with other symptoms such as syncope, dyspnea, or palpitation were regarded as showing no chest pain.

CCTA

Image Acquisition Protocol

All subjects received sublingual nitroglycerin (0.1 mg per dose; Nitroglycerin Inhaler, Jingwei Pharmacy Co, Ltd, Jinan, China) 5 minutes before CCTA acquisition. Beta-blockers were not administered to any of the subjects. All CT examinations were performed on a second-generation dual-source CT system (Somatom Flash, Siemens Healthineers, Forchheim, Germany). Data for all patients were acquired with an adaptive prospectively ECG-triggered sequence at

 https://doi.org/10.3348/kjr.2019.0230

a 30–80% R-R interval. Acquisition parameters were set as follows: detector collimation, 64 x 2 x 0.6 mm; gantry rotation time, 280 ms; effective tube current–time product, 370 mAs per rotation; and tube voltage, 100–120 kVp. All patients received 60 mL of iopromide (Ultravist 370 mg I/mL, Bayer Schering Pharma, Berlin, Germany) via injection into an antecubital vein using a 20-gauge catheter at a flow rate of 5 mL/s. Contrast administration was immediately followed by 40 mL of saline solution injected at 5 mL/s. The bolus tracking technique was employed by placing a region of interest in the aortic root to detect bolus arrival. Image acquisition began 4 seconds after an attenuation threshold of 100 Hounsfield units was achieved.

Image Interpretation

Image quality was graded using a four-point Likert scale (4 = excellent, no significant artifact; 3 = good, mild artifact; 2 = acceptable, moderate artifact present, but image still interpretable; and 1 = not evaluable) using consensus readings obtained by two observers with 18 and 8 years of experience in interpreting CCTA findings (22). All measurements were performed on a dedicated workstation (Syngo.via, Siemens Healthineers). We recorded proximal vessel morphology (9), take-off angle (23), take-off level (6), take-off type, intramural course, % proximal narrowing with minimum diameter/area, length of narrowing, minimum luminal area (MLA) at systole and diastole, and vessel compression index (9). Detailed measurement methods were as follows: 1) Proximal vessel morphology was categorized as "oval" (< 50%) or "slit-like" narrowing (≥ 50% reduction in minimum diameter compared with the normal distal reference segment) at a cross-sectional view perpendicular to the centerline course of the artery (24). 2) Take-off angle in diastole was assessed on the axial or axial-oblique views through the aortic root at the level of the anomalous origin location in diastole (23). 3) Take-off level was determined based on the relationship with the lowest level of the pulmonary valve (PV) in the coronary plane, i.e., "above PV" indicates that the RCA ostium originates above the level of the PV (6). 4) Take-off type was defined as a separate, shared, or branch vessel according to the relationship between the origin of the RCA and the left main coronary artery. 5) Intramural course (i.e., within the aortic wall) was categorized as present or absent with (a) proximal vessel narrowing, (b) acute take-off, and (c) separate ostium of the vessel from the aorta. We also included direct visualization of the vessel within the aortic wall and the absence of adjacent epicardial fat (9). 6) % proximal narrowing equaled (1-minimum diameter / maximum diameter) x 100% and lumen diameters obtained in the double oblique view, considering the maximum and minimum diameters of the vessel at the most narrowed proximal location and the distal reference location using the smallest available slice thickness. 7) Length of narrowing was expressed as the centerline length of vessel narrowing shown in the double oblique and curved multiplanar views extending from R-ACAOS vessel take-off to the normal distal reference location; given the minimal differences in the length of narrowing between cardiac phases, length of narrowing was only measured in diastole. 8) MLA at systole and diastole was also measured in the double oblique view. To evaluate the degree of RCA proximal compression during cardiac phases, the vessel compression index of the RCA proximal segment was defined as follows: | MLA at diastole - MLA at systole | / max (MLA at diastole, MLA at systole).

CT-FFR Modeling and Measurements

CT-FFR calculations were performed on routine CCTA datasets using a software prototype (cFFR, version 3.0.0, Siemens Healthineers). The software is based on an artificial intelligence deep machine learning platform for noninvasively computing FFR values using existing CCTA data, and the detailed algorithm has been reported in more detail in previous studies (16, 18, 25, 26).

The centerline, lumen, and stenosis definitions in CT-FFR were manually edited by one observer and verified by a second experienced observer. CT-FFR measurements were obtained on the condition that segments with the greatest stenosis should be defined based on where they begin and end. Accordingly, to obtain CT-FFR measurements, we lengthened and broadened the proximal RCA segment toward the aorta to mimic the normal RCA segment until the proximal RCA area was approximately equal to the maximum RCA area. Each CT-FFR measurement was performed three times, and the average value was used for the final analysis. Abnormal values for CT-FFR were defined as ≤ 0.80, and patients were considered to have an abnormal CT-FFR if this threshold was reached in either systole or diastole (16, 27). The location of CT-FFR measurement in R-ACAOS patients with an interarterial course is elaborated in Figure 1H.

Statistical Analysis

Statistical analyses were performed with R version 3.1.1 (R Development Core Team). The Kolmogorov-Smirnov test

https://doi.org/10.3348/kjr.2019.0230

Korean Journal of Radiology
KJR

was conducted to assess the normality of quantitative data. Quantitative variables were expressed as mean ± standard deviation if they were normally distributed, while the median and interquartile range were provided for non-normally distributed data. Categorical variables were analyzed using Pearson's chi-squared test. For normally

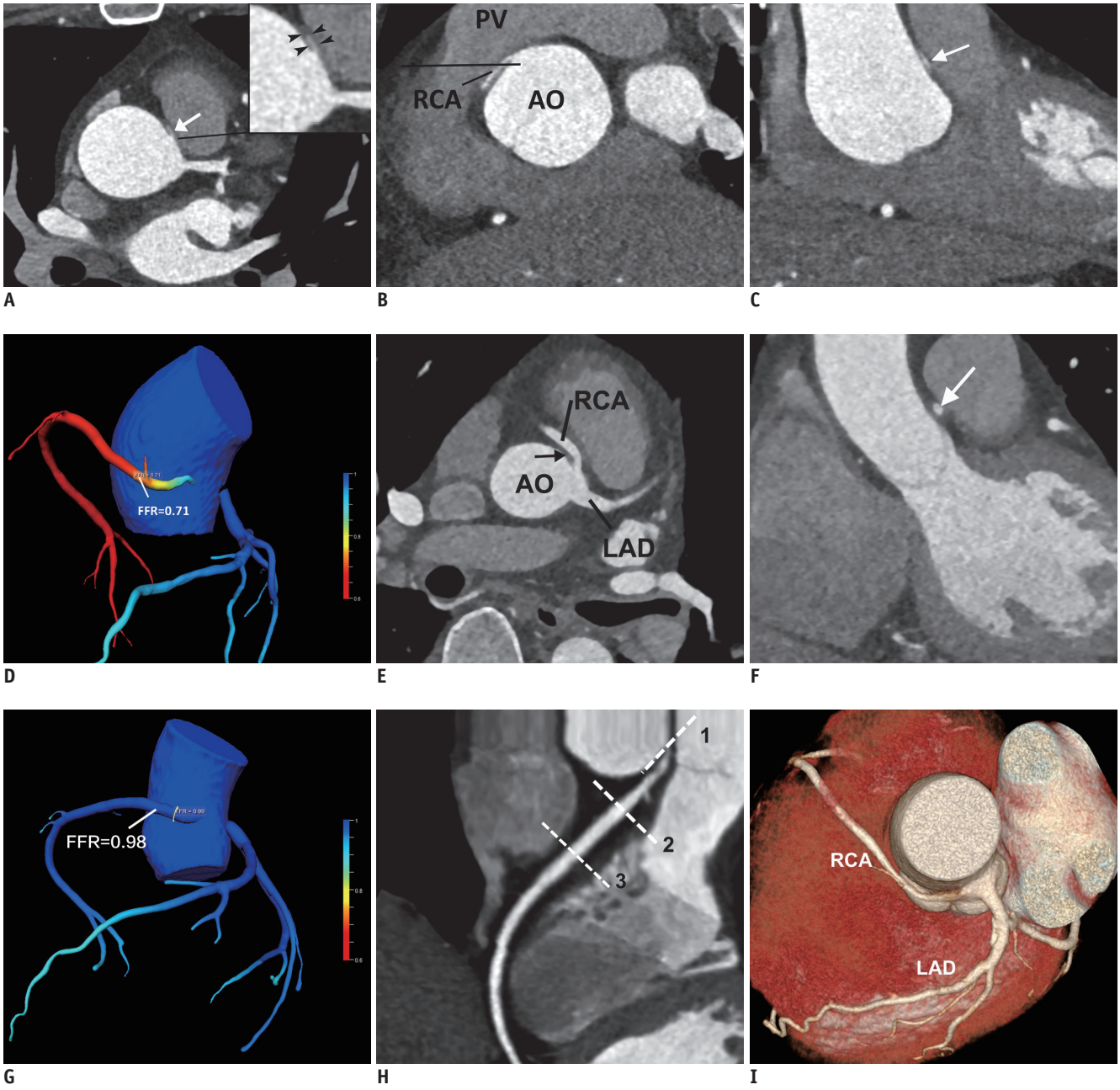

Fig. 1. Representative cases of R-ACAOS with interarterial course R-ACAOS with interarterial course in 54-year-old man presenting with typical angina (A-D) and 49-year-old man without any complaint (E-G). A. Displays separate RCA ostia with acute take-off angle (arrow). Absence of adjacent epicardial fat in magnified view (arrowheads) suggests proximal intramural course of RCA. **B.** Shows take-off level of RCA above PV (line) in coronal view. **C.** Orthogonal cross-sectional image shows classic slit-like RCA proximal segment configuration (arrow). **D.** CT-FFR value of proximal RCA is 0.71, implying ischemia resulting from R-ACAOS with interarterial course. **E, F.** Show R-ACAOS with no intermural course, epicardial fat (arrow in **E**), and oval ostium in orthogonal cross-sections **(**arrow in **F)** with CT-FFR value of 0.98 **(G)**. **H.** Shows location of CT-FFR measurement in R-ACAOS in our study; line 1 is located at RCA ostia, entrance of anomalous origin of RCA, while line 2 lies at exit, indicating lumen narrowing of proximal RCA from line 1 to line 2. CT-FFR values were measured at site of line 3, 1–2 cm distal to lumen narrowing segment of proximal RCA. **I.** Displays volume rendering image of R-ACAOS. AO = aorta, CT-FFR = FFR derived from computed tomographic angiography, FFR = fractional flow reserve, LAD = left anterior descending artery, PV = pulmonary valve, R-ACAOS = RCA from left coronary sinus, RCA = right coronary artery

https://doi.org/10.3348/kjr.2019.0230

distributed data, an independent sample *t* test was used for comparisons between the normal and abnormal CT-FFR groups. The Mann-Whitney U test was used to analyze non-normally distributed data. The Kappa test was conducted to calculate interobserver agreement for CCTA image quality. Patient demographics and anatomical data were analyzed using binary logistic regression analysis and were reported as odds ratio with the corresponding 95% confidence interval. The full model and forward step-wise selection model using the likelihood ratio test with Akaike's information criterion as the stopping rule in multivariable analysis were applied to seek the main predictors of abnormal CT-FFR values in patients with R-ACAOS. Receiver operating characteristic (ROC) analysis was performed to test statistically significant variables for predicting abnormal CT-FFR values in R-ACAOS patients with an interarterial course. Cut-off values were obtained by applying the Youden Index. A p value ≤ 0.05 indicated statistical significance.

RESULTS

Patient Characteristics

Ninety-four patients (61 men [64.9%], 33 women [35.1%]; mean age, 54.4 years; range, 20–83 years) with a heart rate of 69 beats per minute [63–74 beats per minute] were included. Table 1 presents the demographics of patients with CT-FFR ≤ 0.80 versus those with CT-FFR > 0.80. There were no significant differences between the two groups in terms of age, sex, smoking status, and the incidence of diabetes, hypertension, and hypercholesterolemia (all p > 0.05). Of the 94 patients, 11 had typical angina, 10 showed atypical angina, 17 had nonanginal chest pain, 24 reported no chest pain, and 32 were asymptomatic. Of the 94 patients, 21 patients were hospitalized and treated medically for their chief complaint (n = 11) and other causes (i.e., diabetes mellitus, hypertension, etc.) (n = 10), 58 patients were treated medically as outpatients (4 patients refused both hospitalization and invasive coronary angiography), and 15 as outpatients without relevant treatment. Of the 21 patients with clinical follow-up data (median, 12 months; range 1–96 months), 3 were readmitted for persistent chest discomfort despite medical therapy and the 18 remaining outpatients were under continuing medical therapy, of which 12 had reported relief from their previous complaints. A significant difference was found in the hospitalization rate between patients with CT-FFR > 0.8

Table 1. Clinical Features of R-ACAOS Patients with Interarterial Course with Normal and Abnormal CT-FFR Values

Clinical Features	R-ACAOS with Interarterial Course with CT-FFR ≤ 0.80 (n = 17)	R-ACAOS with Interarterial Course with CT-FFR > 0.80 (n = 77)	*P*
Baseline characteristics			
Age, yrs	51.9 ± 11.7	55.1 ± 14.2	0.393
Sex (male), n (%)	14 (82.3)	47 (61.0)	0.096
Diabetes, n (%)	0 (0)	4 (5.2)	1.000
Hypertension, n (%)	4 (23.5)	12 (16.9)	0.479
Smokers, n (%)	6 (35.3)	26 (33.8)	0.904
Hypercholesterolemia, n (%)	5 (29.4)	15 (19.5)	0.348
Chest pain, n (%)			
Typical angina	5 (29.4)	6 (7.8)	0.025
Atypical angina	5 (29.4)	5 (6.5)	0.016
Nonanginal chest pain	0 (0)	17 (22.1)	0.036
No chest pain	2 (11.8)	22 (28.6)	0.222
Syncope	1 (5.9)	3 (3.9)	-
Palpitation	0 (0)	1 (1.3)	-
Dyspnea	1 (5.9)	18 (23.4)	-
Asymptomatic	5 (29.4)	27 (35.1)	0.656
Other tests, n (%)			
CK/CK-MB abnormalities	5 (10.6)	1 (2.1)	0.001
ST-T changes in ECG	2 (11.8)	6 (7.8)	0.633

CK = creatine kinase, CT-FFR = fractional flow reserve derived from computed tomographic angiography, ECG = electrocardiography, MB = myocardium-brain type, R-ACAOS = right coronary artery from left coronary sinus

https://doi.org/10.3348/kjr.2019.0230

Korean Journal of Radiology
KJR

and those with CT-FFR ≤ 0.8 (p = 0.039, 7/17 vs. 14/77).

Anatomical and CT-FFR Features of Patients with R-ACAOS with Interarterial Course

CCTA image quality was rated good or excellent in all 94 patients since we had excluded cases unsuitable for CT-FFR analysis; the kappa value of interobserver agreement for image quality was 0.908. Median computed tomography dose index volume and effective dose in 94 patients with R-ACAOS were 47.9 [19.7–59.5] mGy and 8.2 [3.3–12.2] mSv, respectively. CT-FFR values of the distal location of the lumen narrowing of the proximal RCA were 0.94 [0.88–0.96] (0.91 ± 0.07) in systole and 0.95 [0.87–0.97] (0.91 ± 0.08) in diastole. The distribution of CT-FFR values of the proximal RCA is shown in Supplementary Figure 2. CT-FFR values ≤ 0.80 were found in 18.1% of patients (17/94) in either systole or diastole, and 6.4% (6/94) in both systole and diastole. In the 17 patients, the median CT-FFR value was 0.75 (0.74–0.78). Abnormal CT-FFR values were found in 11.8% of patients (2/17) in systole, 47.1% (8/17) in diastole, and in 41.2% (7/17) during both cardiac phases.

Predictors of Abnormal CT-FFR Values

Anatomical features of R-ACAOS patients with an interarterial course with and without abnormal CT-FFR values are presented in Table 2. Patients with abnormal CT-FFR values were more likely to have a take-off level above the PV, intramural course, slit-like ostium, % proximal narrowing area, and MLA at diastole (all p < 0.05) in univariate analysis. Results from the multivariate analysis to predict abnormal CT-FFR values are illustrated in Figure 2. Full-model multivariate analysis using the screened significant variables from the univariate analysis showed that an RCA take-off level above the PV and a slit-like proximal vessel morphology were the main predictors of abnormal CT-FFR values. Forward step-wise selection of

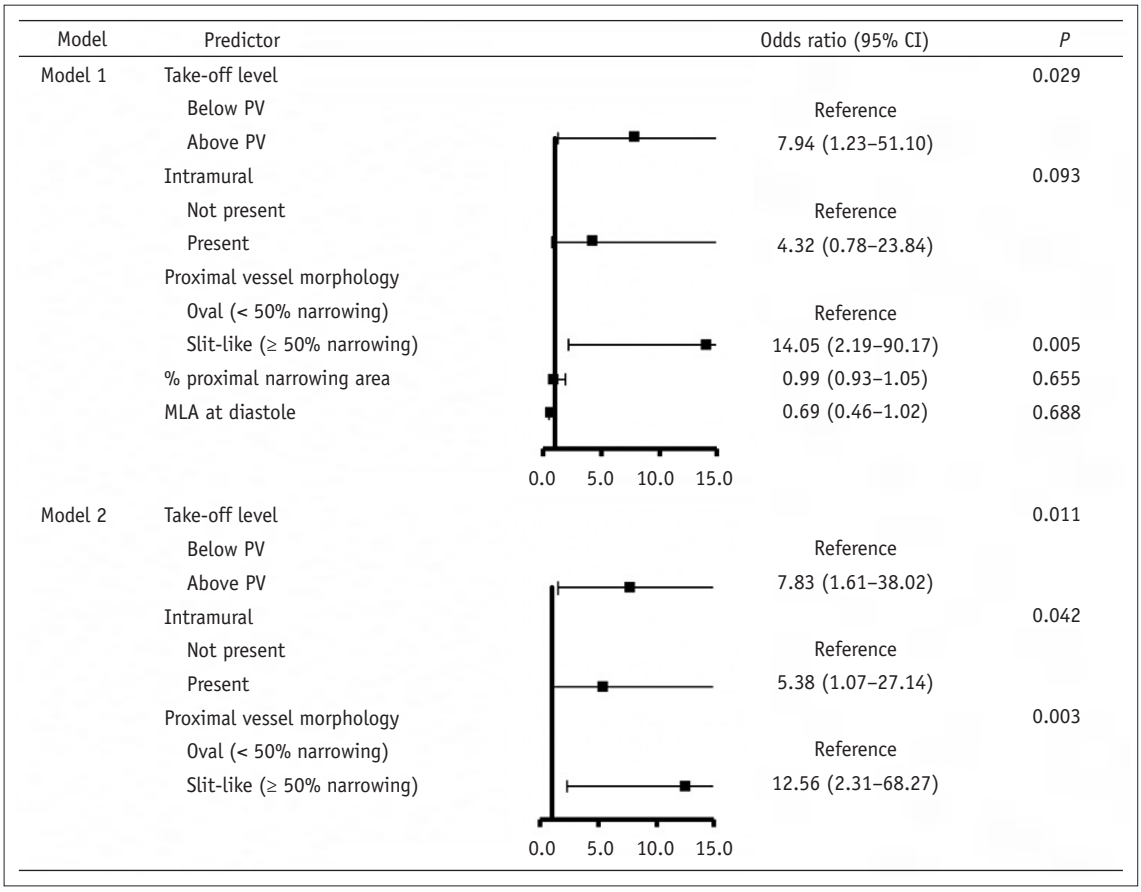

Fig. 2. Multivariate analysis of anatomical features for predicting CT-FFR ≤ 0.80 in interarterial R-ACAOS patients. Model 1 shows full model with screened significant variables from univariate analysis. RCA take-off level above PV and slit-like proximal vessel morphology are found to be main predictors of abnormal CT-FFR values. Forward step-wise selection of model 2 was applied by using likelihood ratio test, which shows that besides RCA take-off level above PV and slit-like proximal vessel morphology, intramural course also contributes to CT-FFR ≤ 0.80 in R-ACAOS patients with interarterial course. CI = confidence interval, MLA = minimum luminal area

https://doi.org/10.3348/kjr.2019.0230

Table 2. Anatomical Features on Coronary CT Angiography in R-ACAOS Patients with Interarterial Course with Normal and Abnormal CT-FFR Values

Anatomical Features	R-ACAOS with Interarterial Course with CT-FFR ≤ 0.80 (n = 17)	R-ACAOS with Interarterial Course with CT-FFR > 0.80 (n = 77)	*P*
Proximal vessel morphology			< 0.001
Oval (< 50% narrowing)	2 (11.8)	59 (76.6)	
Slit-like (≥ 50% narrowing)	15 (88.2)	18 (23.4)	
Take-off angle, degree	9 [6–11]	10 [7–15]	0.145
Take-off level, n (%)			< 0.001
Above PV	14 (82.4)	26 (33.8)	
Below PV	3 (17.6)	51 (66.2)	
Take-off type			
Separate ostia	7 (41.2)	23 (29.9)	0.365
Shared ostia	10 (47.1)	54 (68.8)	
Intramural course, n (%)			< 0.001
Not present	1 (5.9)	53 (68.8)	
Present	16 (94.1)	24 (31.2)	
% proximal narrowing diameter	0.45 [0.37–0.59]	0.39 [0.35–0.50]	0.167
% proximal narrowing area	0.69 [0.51–0.75]	0.52 [0.42–0.61]	0.007
Length of narrowing, mm	24.10 [21.35–33.00]	25.40 [20.55–31.25]	0.837
MLA at systole	4.80 [2.75–6.80]	5.90 [4.55–7.20]	0.092
MLA at diastole	3.80 [1.80–6.15]	5.30 [4.55–6.80]	0.005
Vessel compression index	0.10 [0.01–0.25]	0.08 [0.00–0.17]	0.522

MLA = minimum luminal area, PV = pulmonary valve

model 2 was applied by using the likelihood ratio test with Akaike's information criterion as the stopping rule, which showed that besides RCA take-off above the PV level and slit-like proximal vessel morphology, intramural course also contributed to the prediction of CT-FFR ≤ 0.80 in R-ACAOS patients with an interarterial course. Figure 1 shows a representative case of R-ACAOS with an interarterial course.

For predicting abnormal CT-FFR using ROC analysis, we further analyzed a take-off level above the PV (model 1), intramural course (model 2), slit-like ostium (model 3), and combinations of two or three variables (models 4, 5, 6, 7) (Supplementary Table 1). The diagnostic performances of different models to predict CT-FFR ≤ 0.80 and their corresponding area under the curves (AUCs) are shown in Supplementary Table 1, and the ROC curves for the different models are shown in Figure 3. Take-off level above the PV combined with the intramural course and slit-like ostium had an accuracy of 0.83 and an AUC of 0.92 for predicting CT-FFR ≤ 0.80 in patients with R-ACAOS with an interarterial course.

Clinical Relevance

The various chest pain categories in patients with R-ACAOS with an interarterial course presenting with either normal or abnormal CT-FFR values are provided in Table 1. Compared to patients with normal CT-FFR values, patients with CT-FFR ≤ 0.80 showed a higher prevalence of typical (29.4% vs. 7.8%, $p = 0.025$) and atypical angina (29.4% vs. 6.5%, $p = 0.016$) and were less likely to have non-anginal chest pain (0 vs. 22.1%, $p = 0.036$). No differences between the groups were found for no chest pain ($p = 0.222$) and asymptomatic status ($p = 0.656$). Significant intergroup differences were found in CK and CK-MB levels ($p = 0.001$), but there was no difference in ECG abnormalities ($p = 0.633$).

DISCUSSION

Noninvasive CT-FFR has been insufficiently studied in the setting of patients with R-ACAOS with an interarterial course. Our investigation found that 18.1% of the patients with R-ACAOS with an interarterial course had abnormal CT-FFR values. Take-off level above the PV, intramural course, and a slit-like ostium were the main predictors of abnormal CT-FFR values. Importantly, patients with abnormal CT-FFR values had a higher prevalence of typical angina and atypical angina compared to patients with normal CT-FFR values, suggesting that CT-FFR is a potential tool to gauge the clinical relevance of patients with R-ACAOS with an interarterial course.

https://doi.org/10.3348/kjr.2019.0230

Korean Journal of Radiology
KJR

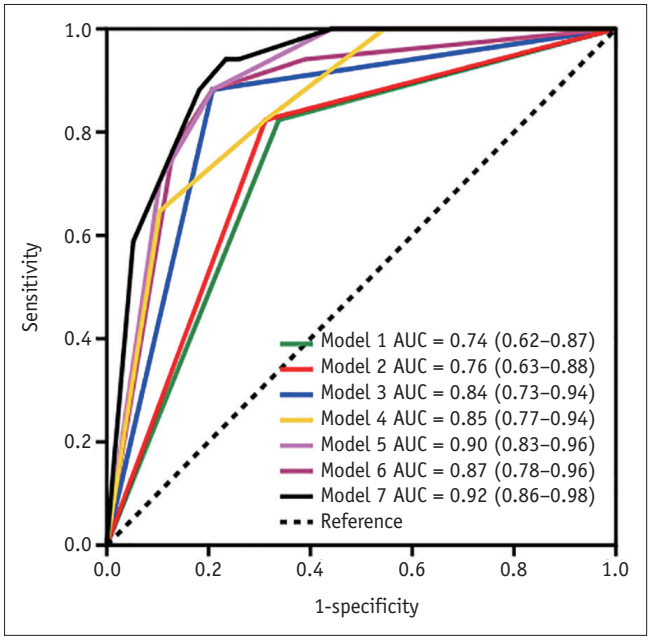

Fig. 3. AUCs for discrimination of CT-FFR ≤ 0.80 in R-ACAOS patients with interarterial course. Model 1: variable 1, take-off level (above PV); Model 2: variable 2, intramural course (present); Model 3: variable 3, proximal vessel morphology (slit-like); Model 4: variables 1 + 2; Model 5: variables 1 + 3; Model 6: variables 2 + 3; Model 7: variables 1 + 2 + 3. AUC = area under curve

Our current study adds to the existing knowledge as the largest investigation of R-ACAOS with an interarterial course on CCTA to date, with a prevalence of 0.29% (121/41580), similar to the weighted prevalence of interarterial R-ACAOS on CCTA in over 100000 patients reported by Cheezum et al. (0.32%) (3). In patients with R-ACAOS with an interarterial course, it is important to evaluate the anatomic features that create a higher risk of restricted coronary blood flow to predict SCD, particularly during exertion (5, 9). However, the mechanism underlying ischemia in ACAOS with an interarterial course has not been fully elucidated. One line of thought is that intense exercise expands the great vessels and in turn compresses the anomalous interarterial coronary artery between the aorta and the pulmonary artery to cause ischemia. Additionally, marked narrowing of the intramural segment has been attributed to segmental hypoplasia, contributing to ischemia (5). Further subclassification is required to identify patients at a higher risk for SCD or ischemia. Lee et al. (6) showed that an acute take-off angle of R-ACAOS with an interarterial course correlates with relative narrowing of luminal diameters at the RCA ostium on CCTA. In our study, all R-ACAOS patients had an acute take-off angle, indicating limited value of this feature in predicting ischemia. Instead, we classified R-ACAOS with an interarterial course into two subtypes to gauge their clinical importance. The patients with a take-off level above the PV in our study were more likely to show abnormal CT-FFR values, supporting the validity of a subclassification based on take-off levels above or below the PV as in Lee et al. (6). Some previous investigations described the significance of an intramural course, but not all R-ACAOS cases with an interarterial course have an intramural component (1, 5). However, identification of an intramural course is important, as only this subset of patients can be treated by coronary unroofing. An intramural course can be confirmed by sophisticated invasive imaging techniques such as intravascular ultrasound or optical coherence tomography. With CCTA, this can be indirectly inferred by the absence of adjacent epicardial fat and a slit-like ostium in orthogonal cross-sections. Notably, although coronary artery diameter is a very important factor (28), only MLA, not minimum lumen diameter (MLD), was included to predict R-ACAOS with CT-FFR ≤ 0.80. Considering the collinearity between MLD and MLA and the fewer contributions of MLD to the hemodynamic abnormality in R-ACAOS in comparison with those of MLA, we left out MLD when analyzing the prediction model with logistic analysis.

In this study, we applied a machine learning-based noninvasive CT-FFR tool in patients with R-ACAOS with an interarterial course to explore the relationship of intracoronary pressures with anatomical features on CCTA and its clinical relevance. The diagnostic performance of this machine learning-based CT-FFR algorithm has been previously investigated and compared to invasive FFR, showing sensitivities and specificities of 85% and 85% by Renker et al. (29), 91% and 96% by Röther et al. (17) and 81.6% and 83.9% by Itu et al. (26) for detecting lesion-specific ischemia. One recent study by Tesche et al. (18) indicated that this machine learning-based CT-FFR algorithm performs as well as the computational fluid dynamics based approach in detecting lesion-specific ischemia. Our study is the first to apply this noninvasive machine learning algorithm to a large sample of R-ACAOS patients with interarterial courses. We found that 18.1% of the patients with R-ACAOS with interarterial courses had abnormal CT-FFR values. Lee et al. (13) examined 37 adult patients with R-ACAOS with an interarterial course by using invasive FFR. They found only one patient (3%) with an abnormal FFR at rest, while only three patients (8%) developed abnormal FFR after dobutamine infusion. Driesen et al. (14) reported that 20% of patients with R-ACAOS with an interarterial course

 https://doi.org/10.3348/kjr.2019.0230

had an abnormal FFR (20%, 5/25), which is similar to our findings. The differences in prevalence among these studies may result from differences in the study populations, and further studies are needed to determine reliable disease rates.

Limitations

Beyond the retrospective nature and relatively small sample size, our study has certain limitations that deserve mention. First, the software prototype (cFFR, version 3.0.0) used in this investigation has not specifically been validated for use with coronary artery anomalies, which could potentially induce measurement errors during model-generation. The CT-FFR cut-off value of this study was established on clinical grounds based on the "prognostic likelihood" of requiring an intervention at the time of angiographic studies of atherosclerotic disease; however, whether it can be used for identifying severe stenosis in carriers of R-ACAOS or whether an CT-FFR cut-off of ≤ 0.80 should be applied also to this condition remains unclear. Thus, further studies are needed to confirm the measurement validity with systematically performed invasive FFR as the reference standard, which is currently infrequently used in this condition. The absence of functional test results may also limit the application of our findings to current risk stratification of R-ACAOS patients with an interarterial course. Second, we did not assess the difference between abnormal CT-FFR values in either one cardiac phase versus those in both phases, so as not to further divide our already small cohort into even smaller sample sizes. Thus, larger populations that allow further subclassification will be required to identify any possible differences. Third, the accuracy of CCTA for measurements of stenosis severity in R-ACAOS patients with an interarterial course may be limited, since the short axis of the stenotic site is usually less than 1 mm in high-risk cases. Fourth, selection bias may be inherent to this population with a comparatively advanced average age of 54.4 years. Most SCDs in these anomalies are reported to occur in children or young athletes rather than in adult survivors who will live with the symptoms but without severe adverse events, so that this latter population is overrepresented in our investigation.

In conclusion, our investigation found that in patients with R-ACAOS with an interarterial course, a take-off level above the PV, intramural course, and a slit-like ostium were more likely to result in decreased CT-FFR values and a higher prevalence of typical angina and atypical angina. Thus, going forward, CT-FFR may have potential as a noninvasive tool for risk stratification in R-ACAOS patients with an interarterial course.

Supplementary Materials

The Data Supplement is available with this article at https://doi.org/10.3348/kjr.2019.0230.

Conflicts of Interest

U. Joseph Schoepf is a consultant for and/or receives research support from Astellas, Bayer, GE, Guerbet, HeartFlow Inc., and Siemens. The other authors have no conflicts of interest to declare.

ORCID iDs

Long Jiang Zhang
https://orcid.org/0000-0002-6664-7224
Chun Xiang Tang
https://orcid.org/0000-0002-0592-7898
Meng Jie Lu
https://orcid.org/0000-0003-4788-7668
Joseph Uwe Schoepf
https://orcid.org/0000-0002-6164-5641
Christian Tesche
https://orcid.org/0000-0002-3584-4284
Maximilian Bauer
https://orcid.org/0000-0002-8179-9250
John Nance
https://orcid.org/0000-0003-3775-4570
Parkwood Griffith
https://orcid.org/0000-0001-7785-5603
Guang Ming Lu
https://orcid.org/0000-0003-4913-2314

REFERENCES

1. Lim JCE, Beale A, Ramcharitar S; Medscape. Anomalous origination of a coronary artery from the opposite sinus. *Nat Rev Cardiol* 2011;8:706-719
2. Angelini P. Novel imaging of coronary artery anomalies to assess their prevalence, the causes of clinical symptoms, and the risk of sudden cardiac death. *Circ Cardiovasc Imaging* 2014;7:747-754
3. Cheezum MK, Liberthson RR, Shah NR, Villines TC, O'Gara PT, Landzberg MJ, et al. Anomalous aortic origin of a coronary artery from the inappropriate sinus of valsalva. *J Am Coll*

Cardiol 2017;69:1592-1608
4. Brothers JA, McBride MG, Seliem MA, Marino BS, Tomlinson RS, Pampaloni MH, et al. Evaluation of myocardial ischemia after surgical repair of anomalous aortic origin of a coronary artery in a series of pediatric patients. *J Am Coll Cardiol* 2007;50:2078-2082
5. Agarwal PP, Dennie C, Pena E, Nguyen E, LaBounty T, Yang B, et al. Anomalous coronary arteries that need intervention: review of pre- and postoperative imaging appearances. *Radiographics* 2017;37:740-757
6. Lee HJ, Hong YJ, Kim HY, Lee J, Hur J, Choi BW, et al. Anomalous origin of the right coronary artery from the left coronary sinus with an interarterial course: subtypes and clinical importance. *Radiology* 2012;262:101-108
7. Angelini P, Vidovich MI, Lawless CE, Elayda MA, Lopez JA, Wolf D, et al. Preventing sudden cardiac death in athletes: in search of evidence-based, cost-effective screening. *Tex Heart Inst J* 2013;40:148-155
8. Shi H, Aschoff AJ, Brambs HJ, Hoffmann MH. Multislice CT imaging of anomalous coronary arteries. *Eur Radiol* 2004;14:2172-2181
9. Cheezum MK, Ghoshhajra B, Bittencourt MS, Hulten EA, Bhatt A, Mousavi N, et al. Anomalous origin of the coronary artery arising from the opposite sinus: prevalence and outcomes in patients undergoing coronary CTA. *Eur Heart J Cardiovasc Imaging* 2017;18:224-235
10. Sayar N, Terzi S, Akbulut T, Bilsel T, Ergelen M, Orhan L, et al. Single coronary artery with subsequent coursing of right coronary artery between aorta and pulmonary artery: fractional flow reserve of the anomalous artery guiding the treatment. *Int Heart J* 2005;46:317-322
11. Dimopoulos K, Di Mario C, Barlis P, Pennell D, Goktekin O, Kaddoura S, et al. Haemodynamic significance of an anomalous right coronary with inter-arterial course assessed with intracoronary pressure measurements during dobutamine challenge. *Int J Cardiol* 2008;126:e32-e35
12. Boler AN, Hilliard AA, Gordon BM. Functional assessment of anomalous right coronary artery using fractional flow reserve: an innovative modality to guide patient management. *Catheter Cardiovasc Interv* 2017;89:316-320
13. Lee SE, Yu CW, Park K, Park KW, Suh JW, Cho YS, et al. Physiological and clinical relevance of anomalous right coronary artery originating from left sinus of Valsalva in adults. *Heart* 2016;102:114-119
14. Driesen BW, Warmerdam EG, Sieswerda GT, Schoof PH, Meijboom FJ, Haas F, et al. Anomalous coronary artery originating from the opposite sinus of Valsalva (ACAOS), fractional flow reserve- and intravascular ultrasound-guided management in adult patients. *Catheter Cardiovasc Interv* 2018;92:68-75
15. Benton SM, Tesche C, De Cecco CN, Duguay TM, Schoepf UJ, Bayer RR. Noninvasive derivation of fractional flow reserve from coronary computed tomographic angiography: a review. *J Thorac Imaging* 2018;33:88-96
16. Tesche C, De Cecco CN, Albrecht MH, Duguay TM, Bayer RR 2nd, Litwin SE, et al. Coronary CT angiography-derived fractional flow reserve. *Radiology* 2017;285:17-33
17. Röther J, Moshage M, Dey D, Schwemmer C, Tröbs M, Blachutzik F, et al. Comparison of invasively measured FFR with FFR derived from coronary CT angiography for detection of lesion-specific ischemia: results from a PC-based prototype algorithm. *J Cardiovasc Comput Tomogr* 2018;12:101-107
18. Tesche C, De Cecco CN, Baumann S, Renker M, McLaurin TW, Duguay TM, et al. Coronary CT angiography-derived fractional flow reserve: machine learning algorithm versus computational fluid dynamics modeling. *Radiology* 2018;288:64-72
19. Zimmermann FM, Kobayashi Y, Mullen WL, Fearon WF. Non-invasive FFRCT revealing severe inducible ischaemia in an anomalous right coronary artery. *Eur Heart J* 2017;38:2569
20. Kawaji T, Shiomi H, Shizuta S, Kimura T. Diagnosis of functional ischemia in a right coronary artery with anomalous aortic origin. *J Cardiovasc Comput Tomogr* 2016;10:188-190
21. Fox K, Garcia MA, Ardissino D, Buszman P, Camici PG, Crea F, et al.; Task Force on the Management of Stable Angina Pectoris of the European Society of Cardiology; ESC Committee for Practice Guidelines (CPG). Guidelines on the management of stable angina pectoris: executive summary: the task force on the management of stable angina pectoris of the European Society of Cardiology. *Eur Heart J* 2006;27:1341-1381
22. Zhang LJ, Wang Y, Schoepf UJ, Meinel FG, Bayer RR 2nd, Qi L, et al. Image quality, radiation dose, and diagnostic accuracy of prospectively ECG-triggered high-pitch coronary CT angiography at 70 kVp in a clinical setting: comparison with invasive coronary angiography. *Eur Radiol* 2016;26:797-806
23. Nasis A, Machado C, Cameron JD, Troupis JM, Meredith IT, Seneviratne SK. Anatomic characteristics and outcome of adults with coronary arteries arising from an anomalous location detected with coronary computed tomography angiography. *Int J Cardiovasc Imaging* 2015;31:181-191
24. Hlatky MA, De Bruyne B, Pontone G, Patel MR, Norgaard BL, Byrne RA, et al. Quality-of-life and economic outcomes of assessing fractional flow reserve with computed tomography angiography: PLATFORM. *J Am Coll Cardiol* 2015;66:2315-2323
25. Duguay TM, Tesche C, Vliegenthart R, De Cecco CN, Lin H, Albrecht MH, et al. Coronary computed tomographic angiography-derived fractional flow reserve based on machine learning for risk stratification of non-culprit coronary narrowings in patients with acute coronary syndrome. *Am J Cardiol* 2017;120:1260-1266
26. Itu L, Rapaka S, Passerini T, Georgescu B, Schwemmer C, Schoebinger M, et al. A machine-learning approach for computation of fractional flow reserve from coronary computed tomography. *J Appl Physiol (1985)* 2016;121:42-52
27. Nørgaard BL, Leipsic J, Gaur S, Seneviratne S, Ko BS, Ito H, et al. Diagnostic performance of noninvasive fractional flow reserve derived from coronary computed tomography angiography in suspected coronary artery disease: the NXT

 https://doi.org/10.3348/kjr.2019.0230

trial (analysis of coronary blood flow using CT angiography: next steps). *J Am Coll Cardiol* 2014;63:1145-1155
28. Park EA, Lee W, Park SJ, Kim YK, Hwang HY. Influence of coronary artery diameter on intracoronary transluminal attenuation gradient during CT angiography. *JACC Cardiovasc Imaging* 2016;9:1074-1083
29. Renker M, Schoepf UJ, Wang R, Meinel FG, Rier JD, Bayer RR 2nd, et al. Comparison of diagnostic value of a novel noninvasive coronary computed tomography angiography method versus standard coronary angiography for assessing fractional flow reserve. *Am J Cardiol* 2014;114:1303-1308

https://doi.org/10.3348/kjr.2019.0230